Deposition of GaSb Films from the Single-Source Precursor $[t\text{-}Bu_2GaSbEt_2]_2$†

Stephan Schulz,* Sonja Fahrenholz, Andreas Kuczkowski, Wilfried Assenmacher, Andreas Seemayer, Alexander Hommes, and Klaus Wandelt‡

Department Chemie, Universität Paderborn, Warburger-Strasse 100, Raum J6.214, D-33098 Paderborn, Germany

Received September 20, 2004. Revised Manuscript Received February 3, 2005

The potential application of $[t\text{-}Bu_2GaSbEt_2]_2$ (**1**) to serve as a *single-source precursor* for the deposition of GaSb films was investigated in detail. Crystalline GaSb films (sphalerite type) were grown on Si(100) by high-vacuum metal−organic chemical vapor deposition between 350 and 550 °C without the use of any carrier gas. The thermal properties of **1** were investigated by differential scanning calorimetry and thermogravimetric analysis/differential thermal analysis, whereas the GaSb films were characterized in detail by means of X-ray diffraction, scanning electron microscopy, transmission electron microscopy, atomic force microscopy, energy-dispersive X-ray spectroscopy, electron energy loss spectroscopy, and Auger electron spectroscopy.

Introduction

Binary antimonides of group 13 elements (Al, Ga, In) generally provide the smallest band gaps of III−V semiconductors (e.g., (eV) 1.60 (AlSb), 0.67 (GaSb), 0.16 eV (InSb)) and show very high electron mobilities. These properties render them very attractive for various electronic and optoelectronic applications. GaSb for instance is used for the construction of light-emitting and light-detecting devices operating in the mid-infrared range, in field effect transistors, in infrared detectors, and in hot electron transistors.[1] Traditionally, GaSb has been grown by metal−organic (MO) MBE and LPE processes.[2] In contrast, the metal−organic chemical vapor deposition (MOCVD) process, which has been established in the last two decades for high-throughput and low-cost fabrication of III−V materials such as binary and ternary group 13 nitrides, phosphides, and arsenides, respectively, is rather problematic for MSb film deposition.[3]

The problems assigned to MSb film growth (M = Al, Ga, In) by MOCVD processes clearly result from the lack of suitable precursors. Group 13 nitrides, phosphides, and arsenides are typically grown by reaction of metal−organic group 13-trialkyls such as MMe_3 or MEt_3 (M = Al, Ga, In) and group 15 hydrides EH_3. The latter produce atomic hydrogen under typical CVD conditions and are consequently used in large excess to reduce the carbon contamination of the resulting materials. In sharp contrast, SbH_3 cannot be used in MOCVD processes due to its low thermal stability.[4] The same is true for primary stibines $RSbH_2$ (R = Me, Et). Consequently, thermally more stable trialkylstibines SbR_3 (R = Me, Et) or $Sb(NMe_2)_3$ have been introduced as Sb sources for the deposition of binary GaSb and InSb films[5] as well as aluminum-based antimonides.[6] Unfortunately, trialkylstibines generally require high deposition temperatures. In addition, detailed studies of Wang et al.[7] on the

† Dedicated to Prof. Martin Jansen on the occasion of his 60th birthday.

* To whom correspondence should be addressed. Phone: (0)5251-602493. Fax: (0)5251-603423. E-mail: stephan.schulz@uni-paderborn.de.

‡ Institut für Physikalische Chemie der Universität Bonn, Wegelerstrasse 12, 53115 Bonn, Germany. Phone: (0)228-732253. Fax: (0)228-732515. E-mail: k.wandelt@uni-bonn.de.

(1) See the following and references therein: (a) Stringfellow, G. B. *Organometallic Vapor-Phase Epitaxy: Theory and Practice*; Academic Press: Boston, MA, 1989. (b) Razeghi, M. *Eur. Phys. J. Appl. Phys.* **2003**, *23*, 149. (c) Mauk, M. G.; Andreev, V. M. *Semicond. Sci. Technol.* **2003**, *18*, 191. (d) Bett, A. W.; Sulima, O. V. *Semicond. Sci. Technol.* **2003**, *18*, 184.

(2) (a) Akahane, K.; Yamamoto, N.; Gozu, S.; Ohtani, N. *J. Cryst. Growth* **2004**, *264*, 21. (b) Xie, Q. H.; Van Nostrand, J. E.; Jones, R. L.; Sizelove, J.; Look, D. C. *J. Cryst. Growth* **1999**, *207*, 255. (c) Grey, R.; Mansoor, F.; Haywood, S. K.; Hill, G.; Mason, N. J.; Walker, P. J. *Opt. Mater.* **1996**, *6*, 69. (d) Ford, J. S.; Howard, F. P.; McGrady, G. S.; Davies, G. J. *J. Cryst. Growth* **1998**, *188*, 144. (e) Mauk, M. G.; Shellenbarger, Z. A.; Cox, J. A.; Sulima, O. V.; Bett, A. W.; Mueller, R. L.; Sims, P. E.; McNeely, J. B.; DiNetta, L. C. *J. Cryst. Growth* **2000**, *211*, 189.

(3) (a) Aardvark, A.; Mason, N. J.; Walker, P. J. *Prog. Cryst. Growth Charact. Mater.* **1997**, *35*, 207. (b) Agert, C.; Lanyi, P.; Bett, A. W. *J. Cryst. Growth* **2001**, *225*, 426. (c) Biefeld, R. M. *Mater. Sci. Eng. Rep.* **2002**, *36*, 105. (d) Dimroth, F.; Agert, C.; Bett, A. W. *J. Cryst. Growth* **2003**, *248*, 265. (e) Möller, K., Kollonitsch, Z.; Giesen, C.; Heuken, M.; Willig, F.; Hannappel, T. *J. Cryst. Growth* **2003**, *248*, 244.

(4) (a) Todd, M. A.; Bandari, G.; Baum, T. H. *Chem. Mater.* **1999**, *11*, 547. (b) Harrison, B. C.; Tompkins, E. H. *Inorg. Chem.* **1962**, *1*, 951. (b) Sugiura, O.; Kameda, H.; Shiina, K.; Matsumura, M. *J. Electron. Mater.* **1988**, *17*, 11.

(5) See the following and references therein: (a) Park, H. S.; Schulz, S.; Wessel, H.; Roesky, H. W. *Chem. Vap. Deposition* **1999**, *5*, 179. (b) Kuczkowski, A.; Schulz, S.; Assenmacher, W. *J. Mater. Chem.* **2001**, *11*, 3241. (c) Berrigan, R. A.; Metson, J. B.; Russell, D. K. *Chem. Vap. Deposition* **1998**, *4*, 23. (d) Subekti, A.; Goldys, E. M.; Paterson, M. J.; Drozdowics-Tomsia K.; Tansley, T. L. *J. Mater. Res.* **1999**, *14*, 1238. (e) Alphandéry, E.; Nicholas, R. J.; Mason, N. J.; Zhang, B.; Möck P.; Booker, G. R. *Appl. Phys. Lett.* **1999**, *74*, 2041. (f) Yi, S. S.; Hansen, D. M.; Inoki, C. K.; Harris, D. L.; Kuan, T. S.; Kuech, T. F. *Appl. Phys. Lett.* **2000**, *77*, 842. (g) Müller-Kirsch, L.; Pohl, U. W.; Heitz, R.; Kirmse, H.; Neumann, W.; Bimberg, D. *J. Cryst. Growth* **2000**, *221*, 611. (h) Yi, S. S.; Moran, P. D.; Zhang, X.; Cerrina, F.; Carter, J.; Smith, H. I.; Kuech, T. F. *Appl. Phys. Lett.* **2001**, *78*, 1358.

(6) (a) Biefeld, R. M.; Allerman, A. A.; Kurtz, S. R. *J. Cryst. Growth* **1997**, *174*, 593. (b) Ramelan, A. H.; Drozdowicz-Tomsia, K.; Goldys, E. M.; Tansley, T. L. *J. Electron. Mater.* **2001**, *30*, 965. (c) Biefeld, R. M.; Kurtz, S. R.; Allerman, A. A. *IEE Proc. Optoelectron.* **1997**, *144*, 271. (d) Giesen, C.; Szymakowski, A.; Rushworth, S.; Heuken, M.; Heime, K. *J. Cryst. Growth* **2000**, *221*, 450.

10.1021/cm048363b CCC: $30.25
Published on Web 03/22/2005

deposition of GaSb films on GaAs substrates between 560 and 640 °C using $GaMe_3$ showed the film growth to be kinetically limited (highest growth rate at 640 °C), whereas the corresponding nitrides and phosphides are typically grown under mass-transport-limited conditions. In contrast, $GaEt_3$ leads to mass-transport-limited film growth due to its lower decomposition temperature (about 100 °C), but its overall growth rate is lower than that for $GaMe_3$. In addition, the GaSb film growth was found to be very sensitive not only to the substrate temperature but also to the Ga/Sb ratio, with the best ratio strongly depending on both the deposition temperature and the precursor combination.[5a]

A possible alternative pathway to overcome the described problems during the growth of binary group 13 antimonides makes use of so-called *single-source precursors*. Typical single-source precursors such as Lewis acid−base adducts $R_3M-ER'_3$ or heterocycles $[R_2MER'_2]_x$ contain the specific elements of the desired material connected by a stable chemical bond *preformed* in a single molecule.[8] They typically show lower metal−carbon bond energies compared to pure group 13 and group 15 trialkyls, allowing lower pyrolysis temperatures,[9] and are less sensitive toward air and moisture. Their capability to serve as precursors for the deposition of group 13 nitrides and phosphides has been demonstrated in the past, but only a very few studies on the deposition of binary group 13 antimonides have been reported. Cowley et al. obtained crystalline MSb films from six-membered heterocycles $[Me_2MSb(t\text{-}Bu)_2]_3$ (M = Ga, In),[10] and our group first reported on the deposition of AlSb films using heterocyclic stibinoalanes $[R_2AlSb(SiMe_3)_2]_2$ (R = Et, *i*-Bu) as well as GaSb films using Lewis acid−base adducts $R_3M-SbR'_3$.[5a,b] Unfortunately, as-described Al−Sb heterocycles lead to an incorporation of Si in the resulting material film due to the presence of silyl substituents in the precursors, whereas Lewis acid−base adducts tend to whisker growth according to the VLS mechanism due to the weak Ga−Sb bond (dissociation!). Consequently, we became interested in the synthesis of completely alkyl-substituted heterocycles and established only recently a novel synthetic route. Distibines $Sb_2R'_4$ react with trialkylgallanes and -indanes MR_3 under Sb−Sb bond cleavage and subsequent formation of the corresponding heterocycles $[R_2MSbR'_2]_x$ (M = Ga, In; x = 2, 3) in almost quantitative yield.[11] This reaction type allows for the first time an extensive ligand variation on both metal centers and the formation of *tailor-made* stibinogallanes and -indanes.

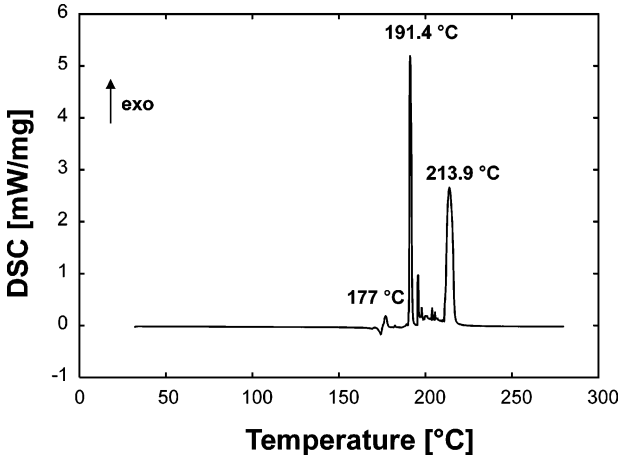

Figure 1. DSC study of [*t*-Bu$_2$GaSbEt$_2$]$_2$ (**1**).

We now report on the thermal properties of [*t*-Bu$_2$GaSbEt$_2$]$_2$ (**1**) as determined by thermogravimetric analysis/differential thermal analysis (TGA/DTA) and differential scanning calorimetry (DSC) studies and its potential capability to serve as a single-source precursor for the deposition of GaSb films by the high-vacuum (HV)-MOCVD process. The resulting films were investigated by X-ray diffraction (XRD), scanning electron microscopy (SEM), transmission electron microscopy (TEM), atomic force microscopy (AFM), energy-dispersive X-ray spectroscopy (EDX), electron energy loss spectroscopy (EELS), and Auger electron spectroscopy (AES).

Results and Discussion

Thermal Properties. A DSC study gives detailed information on the thermal stability of [*t*-Bu$_2$GaSbEt$_2$]$_2$ (**1**) (Figure 1). Heating of **1** in a sealed Al pan to 300 °C with a heating rate of 2 K/min is accompanied by the formation of three major distinguished peaks. The first one at 177 °C agrees well with the melting point of **1** that was determined experimentally to be 180 °C, whereas those at 191 and 213 °C clearly result from stepwise decomposition reactions. Unfortunately, no mass spectroscopy study could be performed to clarify whether the *t*-Bu or the Et substituents are eliminated first. However, since the bond strength of metal−carbon bonds generally decreases with increasing chain length and/or steric branching, the peak at 191.4 °C most likely results from the cleavage of the Ga−C bond.[12] In addition, much smaller peaks around 200 °C point to a more complicated thermal decomposition behavior of **1**, which is not atypical for single-source precursors. However, keeping in mind that the *t*-Bu groups may be eliminated through a β-hydride elimination process, one peak might be assigned to a cleavage of the resulting Ga−H bond.

According to the DSC study, the decomposition of **1** is finished at about 225 °C, proving its thermal stability to be

(7) (c) Wang, C. A.; Salim, S.; Jensen, K. F.; Jones, A. C. *J. Cryst. Growth* **1997**, *170*, 55.

(8) See the following and references therein: (a) Cowley, A. H.; Jones, R. A. *Angew. Chem., Int. Ed. Engl.* **1989**, *28*, 1208. (b) Maury, F. *Adv. Mater.* **1991**, *3*, 542. (c) Fischer, R. A. *Chem. Unserer Zeit* **1995**, *29*, 141. (d) Sauls, F. C.; Interrante, L. V. *Coord. Chem. Rev.* **1993**, *128*, 193. (e) Jones, A. C. *Chem. Soc. Rev.* **1997**, 101. (f) O'Brien, P.; Haggata, S. *Adv. Mater. Opt. Electron.* **1995**, *5*, 117.

(9) MOMBE experiments clearly showed the highest growth rates for the deposition of GaSb films from Et_3Ga and Sb_4 at 600 °C. See the following and references therein: Ford, J. S.; Howard, F. P.; Davies, G. J. *J. Cryst. Growth* **1998**, *188*, 159.

(10) Cowley, A. H.; Jones, R. A.; Nunn, C. M.; Westmoreland, D. L. *Chem. Mater.* **1990**, *2*, 221.

(11) (a) Kuczkowski, A.; Schulz, S.; Nieger, M.; Saarenketo, P. *Organometallics* **2001**, *20*, 2000. (b) Kuczkowski, A.; Fahrenholz, S.; Schulz, S.; Nieger, M. *Organometallics* **2004**, *23*, 3615.

(12) For instance, Sb−carbon bond strengths for several triorganostibines decrease in the following order: Me_3Sb (233.9 kJ/mol) > $(vinyl)_3Sb$ (205 kJ/mol) > *i*-Pr_3Sb (126.8 kJ/mol) > $(allyl)_3Sb$ (90.4 kJ/mol). Jones, A. C.; O'Brien, P. *CVD of Compound Semiconductors*; VCH: Weinheim, Germany, 1997; p 146. Slightly different values are given in the *Handbook of Chemistry and Physics*, 78th ed.; Lide, D. R., Ed.; CRC Press: New York, 1997; pp 9−67: Me_3Sb (255 ± 17 kJ/mol) > Et_3Sb (243 ± 17 kJ/mol).

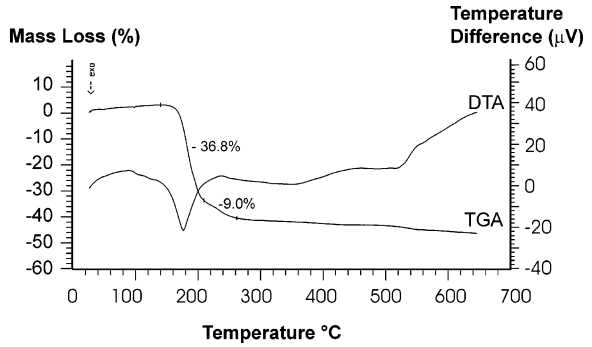

Figure 2. TGA/DTA study of [*t*-$Bu_2GaSbEt_2$]$_2$ (**1**).

rather low. However, it can also clearly be seen that **1** is stable up to its melting point of 177 °C. This is an important finding since a CVD precursor generally has to be thermally stable up to its sublimation temperature to guarantee to be transferred without any decomposition into the gas phase. **1** sublimes without any sign of decomposition at 125 °C at a pressure of 2×10^{-5} mbar.

A TGA/DTA study of **1** (heating rate 10 K/min, open Al_2O_3 pan, carrier gas Ar) is shown in Figure 2. The main mass loss starts at 170 °C and is finished at about 250 °C, which is higher than observed in the DSC study. These findings may be explained by the different heating rates used (2 K/min (DSC) vs 10 K/min (TGA)) and the different heating conditions (sealed pan (DSC), open pan (TGA)).[13] The overall mass loss observed within this temperature range is 45.8%. However, the small temperature window between the melting point (177 °C) and decomposition onset temperature (about 190 °C; see the DSC curve) obviously leads to some mass loss due to volatilization of **1** as is shown by the TGA curve (mass loss even below 190 °C). Therefore, the observed mass loss cannot be directly compared to the calculated mass loss of 47.3% which would be expected due to the direct decomposition of **1** into GaSb. In fact, EDX studies of the solid residue after a TGA/DTA experiment (heated to 600 °C) showed a very inhomogeneous distribution of Ga and Sb within the material formed. Only some single particles showed an almost 1/1 molar ratio, whereas by far the most particles investigated showed a statistic composition from Ga-rich (95% Ga, 5% Sb) to Sb-rich (98% Sb, 2% Ga). These results clearly indicate **1** not to decompose straightforward to give GaSb under these specific conditions.

Film Growth Conditions. CVD studies were performed in a cold wall HV-MOCVD reactor at a working pressure of 5×10^{-5} mbar in the temperature range from 350 to 550 °C without the use of any carrier gas. **1** sublimes at 2×10^{-5} mbar at 125 °C and withstands heating to 170 °C without suffering any decomposition as was expected due to the results of its thermal analyses (DSC, TGA/DTA). To obtain a maximum flow rate of **1** under the as-described CVD conditions, both the flask with 150 mg of the precursor and the glass line to the Si(100) substrate were heated to 160 °C with a heating mantle. No sign of decomposition was observed on the glass walls. The film deposition time was kept constant at 30 min. Due to the presence of native oxide on Si(100) an epitaxial film growth was not expected. The chemical composition, the crystallinity, and the surface morphology of as-deposited material films were found to strongly depend on the substrate temperature.

(13) The steady but slight mass increase (about 2%) between ambient temperature and 150 °C is a simple heating effect (buoyancy of the pan) since no baseline correction was applied. In addition, moisture absorption and surface oxidation reactions of **1**, which was transferred into the chamber through the air, cannot be excluded.

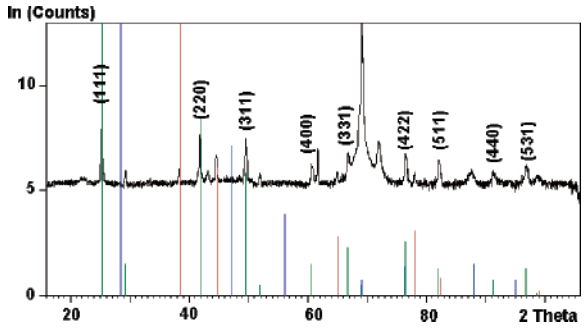

Figure 3. XRD pattern of material films grown on Si(100) at 500 °C from precursor **1**: blue lines, Si substrate reflections; green lines, GaSb reflections (JCPDS File 070215); red lines, reflections of the Al sample holder.

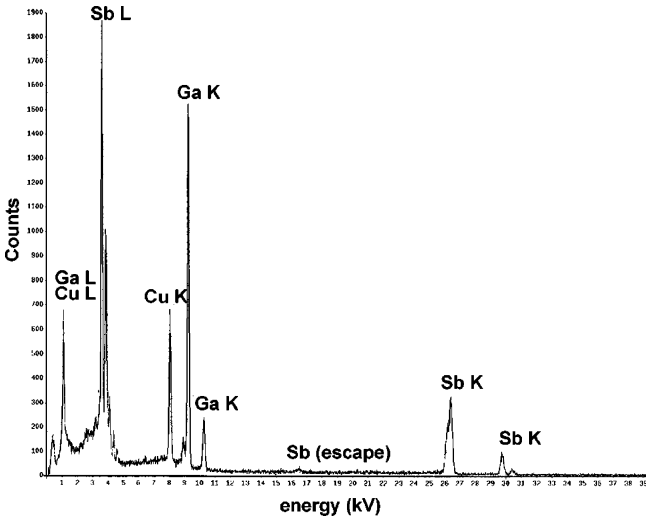

Figure 4. EDX spectrum of a GaSb film grown at 500 °C (Philips CM30, 300 kV, Ge detector). Cu signals are caused by the sample holder grid.

XRD Studies. X-ray diffraction studies of the resulting GaSb films grown on Si(100) at 400, 450, 500, and 550 °C showed reflections due to the presence of crystalline GaSb (sphalerite type), whereas films deposited below 400 °C showed no distinguished reflection due to the presence of any crystalline material.[14] Figure 3 displays a powder pattern (raw data) as-obtained from a film deposited at 500 °C.

The pattern is drawn on a logarithmic scale; otherwise only the strong Si reflection at $2\theta = 69°$ would be visible. Characteristic reflections due to sphalerite-type GaSb clearly prove the formation of crystalline GaSb films. These reflections match JCPDS File 070215 (green), and the lattice parameter of GaSb was refined to 609.51(5) nm.[15]

(14) Annealing of a film that was deposited at 350 °C for 2 h at 500 °C resulted in the formation of broad reflections due to the presence of crystalline GaSb.

(15) In addition, peaks due to Si (substrate, blue) and Al (sample holder, red) are observable. The small peaks at 43.5°, 62°, and 72° could not be assigned to any other possible material such as Ga, Sb, Ga_2O_3, Sb_2O_3, and SiO_2. However, since the XRD pattern was drawn on a logarithmic scale, it cannot be excluded that these peaks may arise from very low impurities of the substrate or the substrate holder.

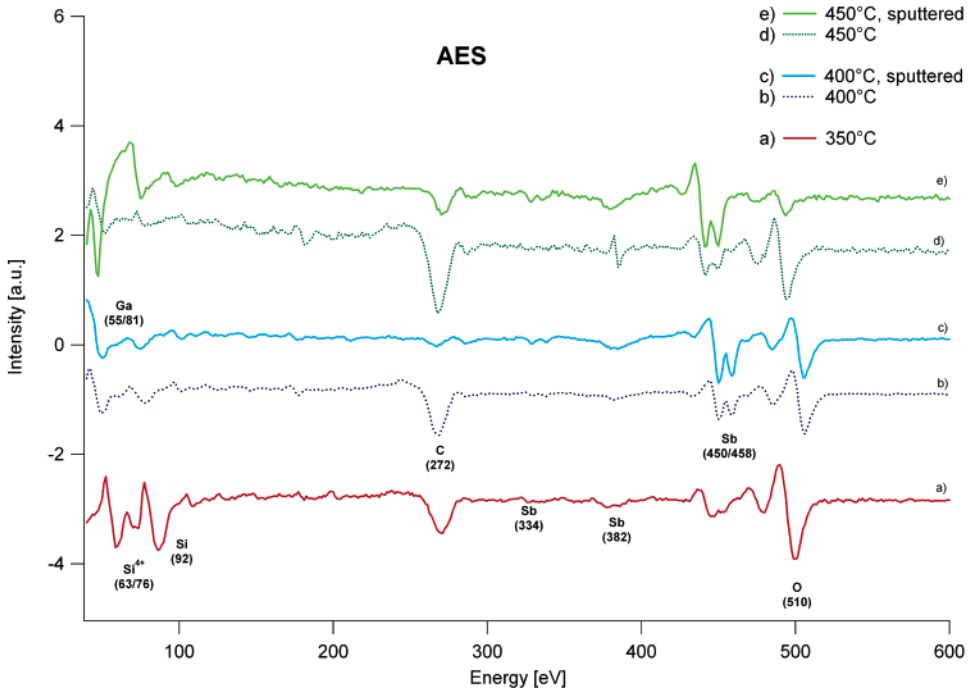

Figure 5. AES spectra of GaSb films grown on Si(100) at (a) 350 °C, (b) 400 °C, and (d) 500 °C, as well as subsequently argon ion sputtered (20 min; c, e).

The substrate temperature was found to play a key role in the density of the resulting films. Those deposited at higher temperature (450, 500, and 550 °C) are more dense, leading to more intense reflections, whereas those deposited in the same time at lower substrate temperatures (350 and 400 °C) are more porous. These results most likely indicate higher decomposition rates of the precursor with increasing temperature as is typical for kinetically controlled film growth processes.

EDX Studies. On the basis of XRD studies, the presence of some amorphous phases/materials coexisting in the layer generally cannot be excluded. To investigate the elemental composition of the material films in detail, EDX and AES analyses were performed on different films (Figure 4).

EDX spectra as-recorded on a transmission electron microscope from films that were deposited between 350 and 550 °C showed comparable results. Quantification of several spectra both obtained from single crystallites and larger areas showed equal amounts of Ga and Sb. The Sb/Ga molar ratio typically ranges from 1.0 to 1.03,[16] indicating the formation of slightly Sb-rich material. In addition, peaks due to the presence of Si (substrate) were observed. Unfortunately, EDX is not very valuable for the determination of light elements such as carbon and oxygen. Consequently, detailed AES studies were performed to determine any contamination of the films with these two elements both on the surface and throughout the material film (sputtering experiments).

AES Studies. AES spectra of GaSb films deposited between 350 and 550 °C show clear signals for gallium (55/81 eV), silicon (63/76; 92 eV), and antimony (334, 382, and 450/458 eV). In addition, they show some contamination with oxygen (510 eV) and carbon (272 eV). AES spectra of material films deposited between 350 and 450 °C are displayed in Figure 5.

Even though the film thicknesses of each film are comparable (1−1.5 μm), only the one deposited at 350 °C shows strong Si signals due to reflections of the substrate. This finding points to an incomplete coverage of the Si substrate and a porous film structure. In contrast, the spectra of the films deposited at 400 and 450 °C show much less Si, suggesting the formation of a more dense film structure with increasing substrate temperature.

Of particular interest is the relative Sb/C intensity as a function of substrate temperature and sputter treatment. With increasing deposition temperature, the Sb/C intensity ratio slightly increases as can be seen in Figure 5. These findings indicate a more complete decomposition of the precursor with increasing substrate temperature as is typical for kinetically controlled film growth processes. However, Ar sputtering of the films for 20 min leads to a significant decrease of both the C and O intensities (increasing Sb/C and Sb/O intensity ratios), proving both elements almost exclusively to be present as a surface layer.[17] The carbon contamination most likely results from a deposition of precursor molecules from the gas phase on the film at the end of the film growth process, giving a surface layer of incompletely decomposed precursor molecules, or from some absorption of environmental C sources during the transport of the film into the

(16) The spectra were quantified using the Sb L and Ga K lines with calculated weight percentages of 36.41 and 63.59 for Ga and Sb in GaSb.

(17) The Ar beam hit the film surface with an angle of 15° from the vertical alignment. Assuming each Ar ion removes one atom from the surface, the sputter rate can be estimated to be about 0.01 monolayer/s (=3 nm in 20 min). Since the films show a thickness profile (polycrystalline material) and since no vertical alignment of the Ar beam was used, no uniform removal of the surface layer takes place, which may explain to some extent the presence of a very small O and C concentration even after Ar bombardment.

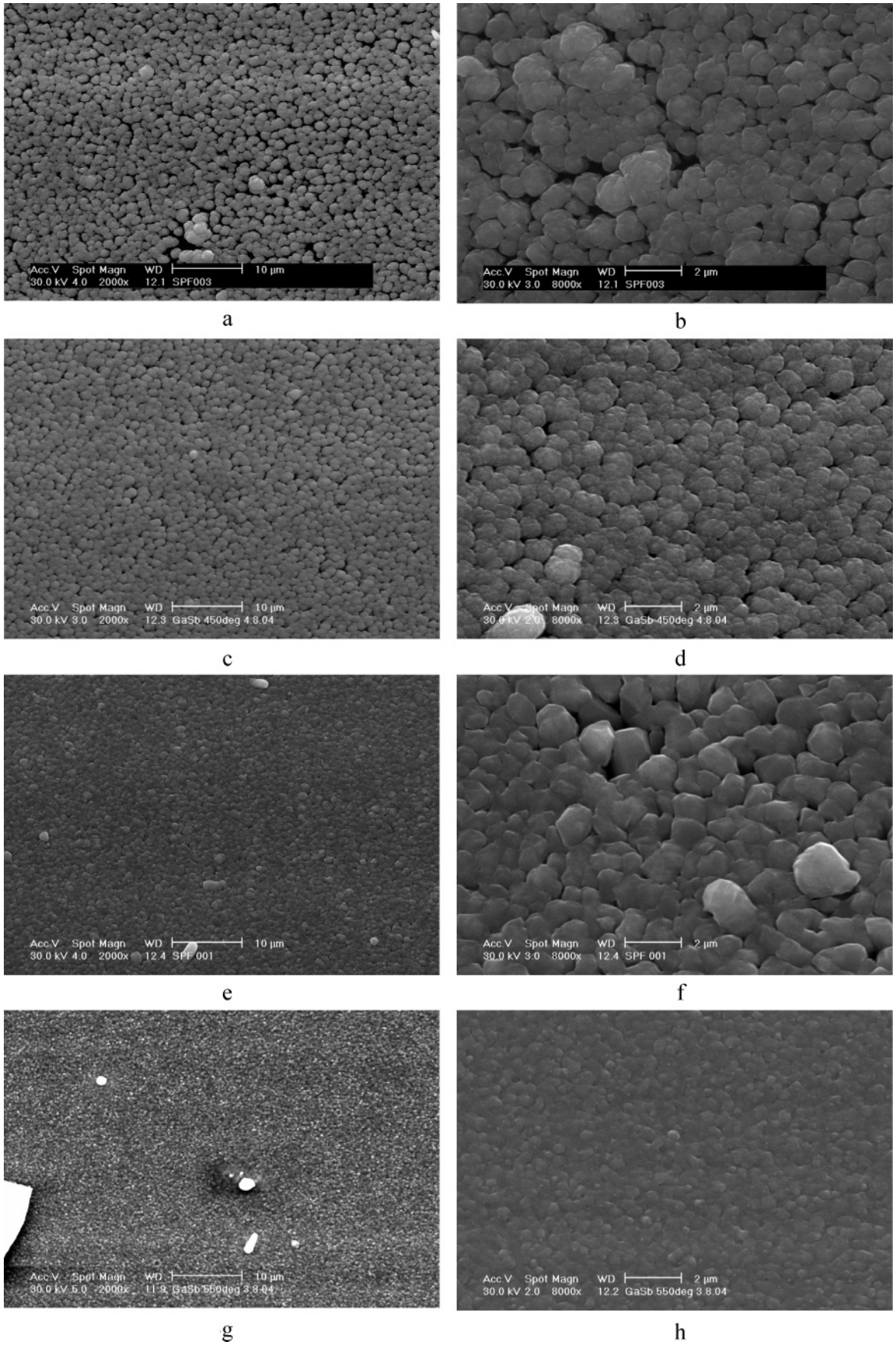

Figure 6. SEM images displaying the surface morphology of GaSb films grown at 400 °C (a, b), 450 °C (c, d), 500 °C (e, f), and 550 °C (g, h).

AES chamber. This surface layer consequently can be removed by Ar sputtering, giving a pure surface of the GaSb film. In contrast, the O contamination clearly results from surface oxidation reactions.[18]

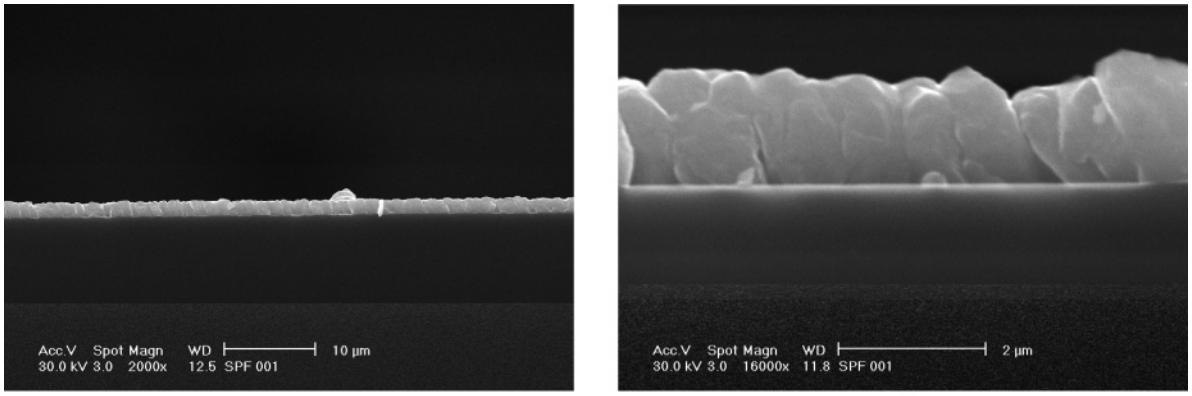

Figure 7. SEM cross-section images of the GaSb film deposited at 500 °C.

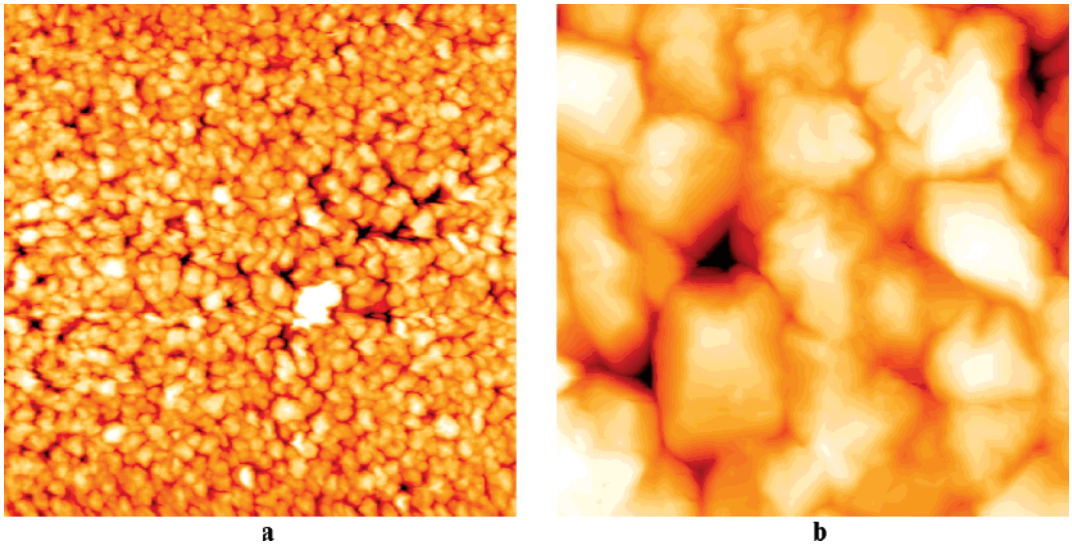

Figure 8. AFM images [(a) 6.3 μm × 6.3 μm and (b) 400 nm × 400 nm] of an unsputtered GaSb film grown at 500 °C.

SEM Studies. The morphology of the GaSb thin films was examined by SEM. Figure 6 shows images of films with different magnifications, which were grown between 400 and 550 °C (50 °C steps).

The films obtained show very homogeneous morphologies. However, the coatings of the GaSb films show an increased density with increasing substrate temperature. Consequently, the film deposited at 550 °C is the densest one, whereas those deposited at lower temperatures are more porous.[19] The size of the GaSb crystallites found for each film is very uniform. The homogeneous film growth can also be seen from Figure 7, showing cross-section views of a film grown at 500 °C. Its polycrystalline character can easily be seen. The presence of GaSb particles of almost equal sizes indicates a three-dimensional island growth, referred to as Vollmer−Weber growth. Small GaSb clusters, which are formed due to the decomposition of the precursor molecules **1**, are nucleated at the substrate surface and finally grow together and build a continuous and homogeneous GaSb film, which is about 1.5 μm thick. Since the decomposition rate of the precursor increases with increasing temperature (kinetically controlled growth regime), more material is deposited at the substrate and the density of the resulting GaSb films increases with increasing substrate temperature.

AFM studies obtained from measurements in the contact mode clearly verified these results. Figure 8 displays AFM images as-obtained from a GaSb film deposited at 500 °C. The homogeneous film growth can clearly be seen (Figure 8a). In higher magnification, cubic-shaped crystals are observable (Figure 8b). The thickness of the film was determined to be about 1 μm as can be seen in Figure 9.

TEM Studies. To investigate the morphology of the GaSb particles in more detail, TEM studies of several films were performed. For this purpose, GaSb particles were simply scratched from the substrate.[20] Typical bright-field images of the particles deposited at 500 °C are shown in Figure 10.

Unfortunately, only a few crystals are thin enough to be electron-transparent. Typically, agglomerations containing several crystals sticking together are observed. The elemental composition within the films as-obtained from EDX studies was confirmed by EEL spectroscopy, also showing Sb/Ga ratios in the particles ranging from 1.0 to 1.03. The Ga and

(18) The GaSb films were handled in air when transferred to the AES chamber.
(19) Unfortunately, X-ray reflectometry could not be performed due to the lack of suitable instrumentation.
(20) The adhesion of the GaSb film at the substrate is not very good, so the particles can easily be removed from the substrate surface. The poor adhesion most likely is the reason for the Vollmer−Weber-like growth.

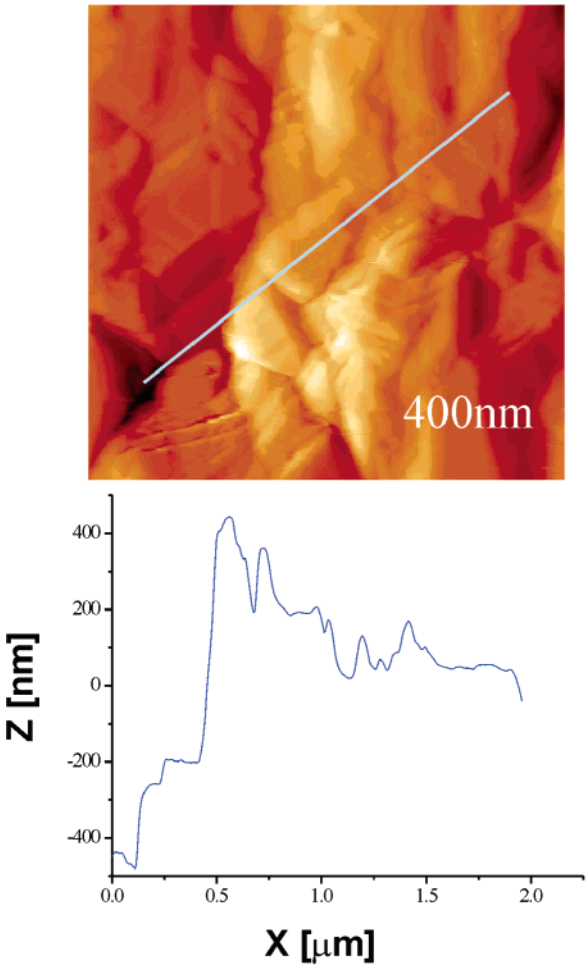

Figure 9. AFM image showing the thickness of the deposited GaSb film.

Sb distribution within the particles is very uniform as was confirmed by element mapping. In addition, EELS was performed to determine the carbon and oxygen content of the particles. Even after background correction and deconvolution against multiple scattering, the carbon concentration in any particle analyzed was below the detection limit of EELS. This agrees very well with the results as-obtained from the AES studies, which suggested carbon to be present only as a thin surface layer but not throughout the material. In addition, EELS clearly proved the presence of oxygen at the surface of each crystal.[21] This is reasonable due to the sensitivity of GaSb toward surface oxidation. Since the sample preparation was not performed under an inert gas atmosphere, such a process is very likely.

Conclusions

GaSb films were grown in high-vacuum conditions from the single-source precursor [*t*-$Bu_2GaSbEt_2]_2$ (**1**) using a cold wall MOCVD reactor in the absence of any carrier gas. Crystalline GaSb films of sphalerite type were obtained between 400 and 550 °C, whereas below 400 °C only amorphous material was formed. The film density was found to increase with increasing substrate temperature. In all experiments, slightly Sb-rich GaSb films were obtained. As-prepared films showed some O and C contaminations, which were proven by sputtering experiments and by EELS to be present only as surface layers.

The deposition studies clearly demonstrate the potential applicability of **1** to serve as a single-source precursor for the growth of crystalline GaSb films. In particular the absence of any carbon contamination within the material film and the very low decomposition temperatures render **1** very attractive for further MOCVD studies. Studies on the deposition of epitaxial films will be performed soon.

Experimental Section

All manipulations with metal−organic compounds were performed in a glovebox under a N_2 atmosphere. Compound **1** was synthesized by a literature method.[11]

MOCVD Experiments. Film growth experiments were carried out in high-vacuum conditions in a cold wall CVD reactor. GaSb was deposited on Si(100) substrates, which were previously degreased with 2-propanol, rinsed with distilled water, and treated with hydrofluoric acid for 1 min. The substrate was rinsed again with distilled water and then treated with dry nitrogen prior to film

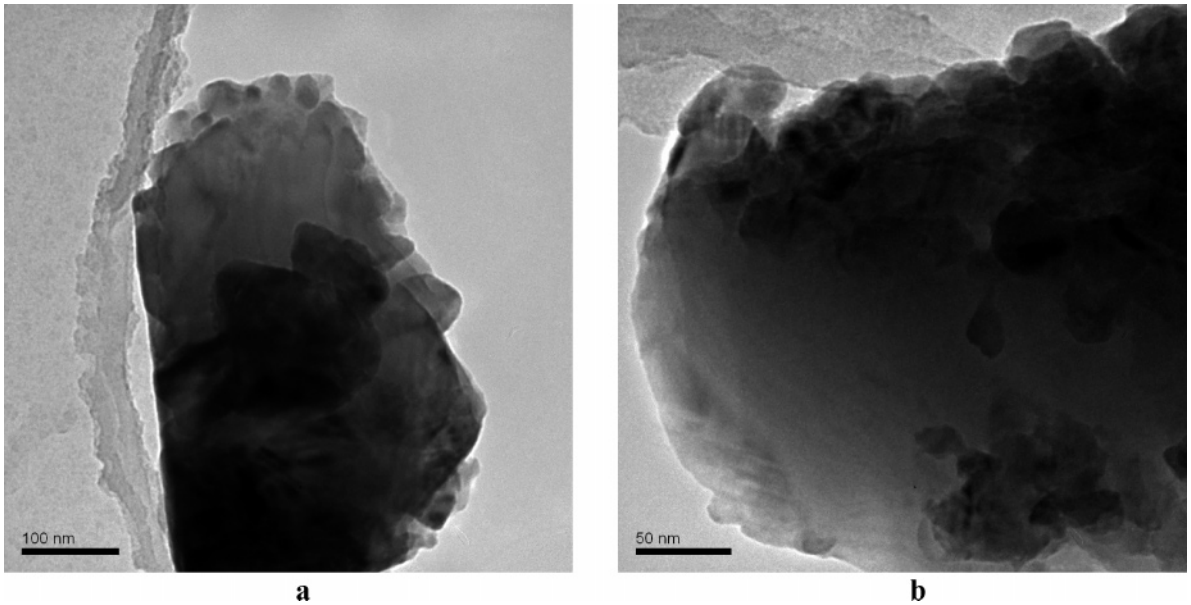

Figure 10. Bright-field images of GaSb particles as found in TEM studies.

deposition. After the substrate was loaded onto the substrate holder, the reactor was evacuated to a pressure of 10^{-6} mbar for 1 h. During this time the substrate was heated to 500 °C using a resistance furnace, and the temperature was measured by a thermocouple, which was placed directly under the substrate. The precursor (0.15 g) was loaded into a glass tube which was then attached to the CVD apparatus. The temperature of the substrate and the pressure in the reactor were adjusted before film growth. The pressure was below 5×10^{-5} mbar during the film growth. After deposition, the system was cooled to room temperature under a vacuum.

XRD patterns of the resulting GaSb films were recorded on a Philips 1050 diffractometer with an AFM secondary monochromator using Cu Kα radiation. They were also characterized by means of SEM studies using a Philips XL20 (W-filament) equipped with an EDX device (Noran Voyager, Si(Li)) and TEM using a Philips CM30ST (LaB_6 cathode) at 300 keV equipped with a parallel EEL spectrometer (Gatan P666) or a Philips CM300UT (FEG) at 297 keV equipped with a SlowScan CCD (Gatan, 2K × 2K) and an imaging filter (Gatan GIF200) for recording EEL spectra and energy-filtered images with a second CCD (1K × 1K) at the end of the filter. An HP-Ge EDX detector (Noran Voyager) was present on both transmission electron microscopes for EDX analysis. Sb L and Ga K lines were used for quantification of the EDX data. The Sb/Ga ratio was determined using the "metal-thin-foil method" with *k*-factors (Cliff−Lorrimer method) yielded from calibration of the EDX system with certified GaSb from Aldrich Chemical Co. The samples were prepared on perforated carbon foils without further grinding. The AES measurements were carried out at ambient temperature in a standard ultra-high-vacuum chamber with a base pressure in the range of 10^{-9} mbar. Surface cleaning was achieved by sputtering with argon ions with a beam energy of 2 keV and a current in the range of 5 μA for 20 min. The AFM measurements were performed with a Pico SPM I (Molecular Imaging Corp., Santa Barbara, CA) using a BS-Cont Al cantilever from Budgetsensor with a force constant of 0.2 N/m. All AFM measurements were made under ambient conditions. During the transfer between the CVD reactor and the AES/AFM measurements the samples were stored under ambient conditions in a small glass vessel.

(21) The quantification of EEL spectra uses the intensity of ionization edges in an energy interval of 10−200 eV after the edge. In the given situation with a narrow O K edge and with the Sb M edge present in the same spectrum, only the counts from a 5 eV energy interval can be used, leading to large standard deviations for the results. Oxygen was determined to be present in an amount of ∼1% within thin areas of the samples.

Acknowledgment. We thank the Deutsche Forschungsgemeinschaft (Schwerpunktprogramm 1119), the Bundesministerium für Bildung, Forschung, Wissenschaft und Technik (BMBF), and the Fonds der Chemischen Industrie for financial support of this work.

CM048363B